

Cite this: *Chem. Sci.*, 2021, **12**, 6315

All publication charges for this article have been paid for by the Royal Society of Chemistry

Received 19th March 2021
Accepted 30th March 2021

DOI: 10.1039/d1sc01571k
rsc.li/chemical-science

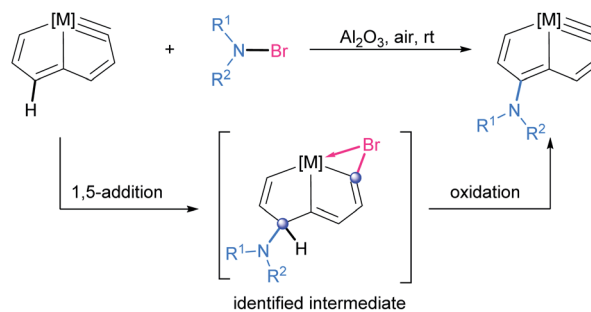
Introduction

The direct C–H amidation of arenes provides an efficient and economical approach to construction of valuable C–N bonds avoiding the use of prefunctionalized aromatic components.¹ Various catalysts and effective amidation reagents have been explored and have led to improvements in the scope of substrates and functional group tolerance.² Activated N–X amide reagents, such as *N*-haloimides or *N*-acyloxyimides, typically undergo homolytic cleavage to generate a nitrogen-centered radical, which can undergo *N*-aryl bond formation.^{3,4} The reactions usually proceed through photoredox catalysis,^{4e,f} and are potential alternatives to the transition metal mediated catalysis assisted by directing groups.

Transition-metal-containing metallaaromatic compounds are analogues of the corresponding organic aromatic compounds,⁵ and have attracted growing interest.^{6–13} Two main strategies have been developed for the construction of the *N*-aryl bond in metallaaromatic compounds. Electrophilic substitution reaction of metallaaromatic compounds is a convenient route to obtain nitro-substituted derivatives,¹⁴ which are useful for further *N*-functionalization.¹⁵ For example, Wright *et al.* synthesized amido-substituted and imido-substituted fused-ring metallabzenes starting from nitro-substituted

iridabenzofurans *via* multiple consecutive reactions.¹⁵ As an alternative, by pre-installation of a functional group on the metallacycle, intramolecular nucleophilic aromatic substitutions and *cine*-substitution reactions can be realized to access *N*-functionalized metallaaromatics.¹⁶ Despite these impressive advances, approaches to amido-substituted metallaaromatic usually require multistep pathways or prefunctionalized starting materials. Direct C–H amidation has emerged as a step- and atom-economical alternative, but is elusive and its successful completion is challenging.

Herein we report the direct amidation of metallaaromatics with *N*-bromoamides and *N*-bromoimides, respectively. A planar Möbius metallaaromatic, osmapentalyne, was employed as a model substrate and a series of *N*-functionalized metlapentalyne derivatives have been synthesized under mild conditions at room temperature (rt) (Scheme 1). The identified 1,5-bromoamidation metallacyclic intermediate suggests that the reaction proceeds a unique pathway involving electrophilic



^aState Key Laboratory of Physical Chemistry of Solid Surfaces, Collaborative Innovation Center of Chemistry for Energy Materials (iChEM), College of Chemistry and Chemical Engineering, Xiamen University, Xiamen 361005, China. E-mail: linyum@xmu.edu.cn; hpxia@xmu.edu.cn

^bShenzhen Grubbs Institute, Department of Chemistry, Southern University of Science and Technology, Shenzhen 518055, China

† Electronic supplementary information (ESI) available: Characterization details of new compounds, crystallographic details, NMR spectra. CCDC 2053993 (S), 2054261 (1), 2054330 (2a), 2054286 (2b), 2054272 (2c), 2054274 (2d), 2054285 (2e), 2054269 (4a) and 2069503 (5). For ESI and crystallographic data in CIF or other electronic format see DOI: 10.1039/d1sc01571k

Scheme 1 Direct amidation of metallaaromatics *via* 1,5-bromoamidated intermediate.



addition and nucleophilic attack. This is quite different from the typical radical process of organic arene C–H amidation involving *N*-haloamide reagents.

Results and discussion

Synthesis and characterization of osmapentalyne 1

We have previously reported some interesting metallaromatics, *i.e.* metallapentalynes containing a metal–carbon triple bond in a five-membered ring, which exhibit the rare planar Möbius aromaticity.^{8b,17} In order to investigate the direct amidation strategy to obtain its *N*-functionalized derivatives, we envisioned that metallapentalyne with relatively electron-deficient groups would participate in the substitution of hydrogen by the amidating reagent. Accordingly, we designed and synthesized the tri-substituted osmapentalyne **1**. Details of the synthesis and characterization are in the ESI (see ESI, p. S4†). As shown in Fig. 1, the metallacycle contains an osmium shared by two fused five-membered rings. The eight atoms (Os1, C1–C7) are coplanar as reflected by the mean deviation of 0.010 Å from the least squares plane and the sum of angles in the fused five-membered rings, which are both 540.0°. The coplanarity as well as the Os–C and C–C bond distances in the fused five membered ring indicates it is a delocalized metallabicyclic compound, which resembles our previously reported aromatic osmapentalynes.^{8b,17}

Direct C–H amidation or imidation of osmapentalyne 1: procedure, scope and characterization of products

We investigated the reactions of osmapentalyne **1** with various amidating reagents (Table 1). When **1** was reacted with *N*-bromophthalimide (NBP) in the presence of aluminium oxide in air at rt for 12 h, complex **2a** was formed in 92% yield. The product **2a** can also be obtained in 81% yield when the reaction mixture was treated with CH₃COONa instead of Al₂O₃ (see ESI, p. S5†). Treatment of compound **1** with *N*-bromosuccinimide (NBS)

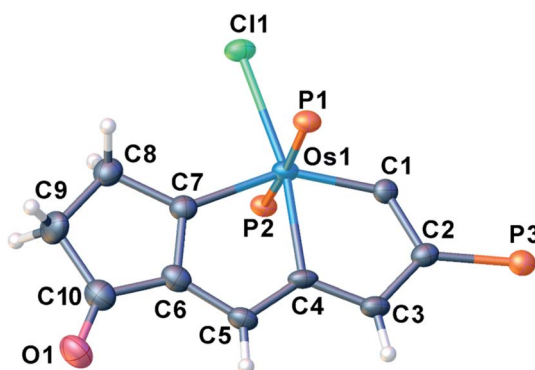


Fig. 1 X-ray crystal structure of the cation of **1** (thermal ellipsoids are set at the 50% probability level and the phenyl groups in the PPh₃ moieties are omitted for clarity). Selected bond lengths [Å] and angles [°]: Os1–C1: 1.858(3), Os1–C4: 2.106(3), Os1–C7: 2.045(3), C1–C2: 1.398(4), C2–C3: 1.398(5), C3–C4: 1.398(5), C4–C5: 1.397(5), C5–C6: 1.410(5), C6–C7: 1.396(5), C4–Os1–C1: 72.31(13), C7–Os1–C4: 75.01(13).

Table 1 Scope of amidation reagents^a

Entry	[N]	Yield ^b (%)	Entry	[N]	Yield ^b (%)
2a		92	2d		80
2b		90	2e		85
2c		93	2f		76
			2g		71

^a Reaction conditions: **1** (0.20 mmol) with *N*-bromocarboxamide (0.60 mmol) and Al₂O₃ (5.0 mmol) in CH₂Cl₂ (10.0 mL) for 12 h at rt in air.

^b Isolated yield. [Os] = OsCl(PPh₃)₂.

under similar conditions led to the formation of **2b** in 90% yield. Complexes **2a** and **2b** were characterized by X-ray crystallographic analysis. As shown in Fig. 2, the metallacyclic

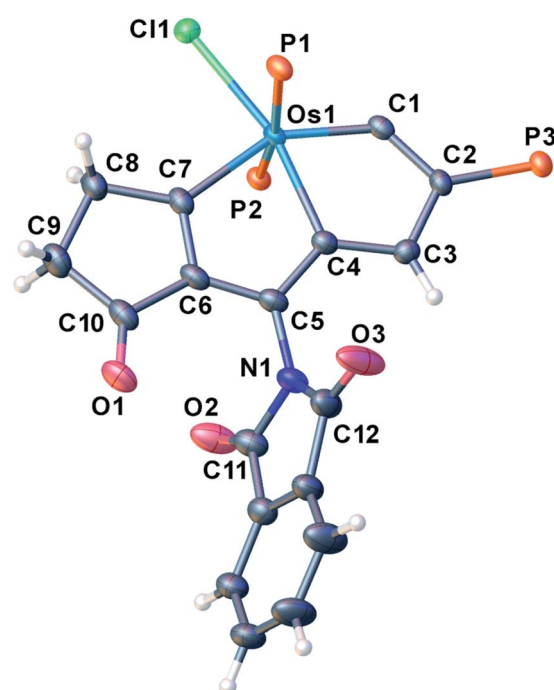


Fig. 2 X-ray crystal structure of the cation of **2a** (thermal ellipsoids are set at the 50% probability level and the phenyl groups in the PPh₃ moieties are omitted for clarity). Selected bond lengths [Å] and angles [°]: Os1–C1: 1.842(2), Os1–C4: 2.111(2), Os1–C7: 2.044(2), C1–C2: 1.404(3), C2–C3: 1.404(3), C3–C4: 1.414(3), C4–C5: 1.397(3), C5–C6: 1.397(3), C6–C7: 1.388(3), C5–N1: 1.430(3), C4–Os1–C1: 72.32(9), C7–Os1–C4: 75.89(9).



skeleton of **2a** is similar to that of **1**, with the exception of the phthalimido substitute attached to C5. The length of the C5–N1 bond (1.430(3) Å) indicates its single-bond character, and is similar to the reported *N*-aryl single bond (1.464(4) Å) in the imide-substituted metallaaromatics.¹⁵ The dihedral angle between the metallabicyclic unit and the imide group is 62.40°. The Os1–C1 bond length (1.842(2) Å) suggests that it maintains the Os≡C triple bond character. The C–C bond lengths (1.388–1.414 Å) in the fused five-membered rings are intermediate between the lengths of C–C and C=C bonds and show no significant bond-length alternation. The planarity and the bond lengths in the fused five membered rings indicate it is a delocalized metallabicyclic compound. All these parameters are consistent with **2a** being a C5-phthalimido-substituted osmapentalyne derivative.

The solid-state structure of **2a** is fully supported by NMR spectroscopy. In the ¹H NMR spectrum, the characteristic signal of H3 (δ = 8.30 ppm) appears in the aromatic region. Carbon C5 bearing the phthalimido substitute has a peak at δ = 140.3 ppm. In the ³¹P{¹H} NMR spectrum of **2a**, only one singlet (δ = –0.18 ppm) is observed for the two PPh₃ ligands, indicating that the two phosphorus atoms are equivalent.

Encouraged by the effective imidation of osmapentalyne with NBP and NBS, we then examined other amidating reagents. *N*-Bromocarboxamides substituted with different groups were subjected to the standard reaction conditions. The methyl, phenyl, benzyl, *n*-propyl and cyclohexyl groups were all well-tolerated, yielding the corresponding products in moderate to excellent yields (71–93%, **2c**–**2g**) (Table 1). Complexes **2c**, **2d** and **2e** have been fully characterized by X-ray crystallographic analysis and all the structures were further supported by NMR spectroscopy and high-resolution mass spectrometry (HRMS) (see ESI p. S44–S53†).

The structural parameters of the fused rings in compound **2c** resemble those in **2a** (Fig. 3). The acetamide group attached at C5 position is indicated by the N1–C5 bond length (1.387(11) Å), which is close to that of the reported *N*-aryl single bond (1.391(4) Å) in osmabenzoxazolone.^{16c} The intramolecular hydrogen bonds N1H···O1 (2.107 Å) and H3···O2 (2.105 Å) were also observed in the acetamide-substituted osmapentalyne.

Investigation of the mechanism: identification of key intermediates and control experiments

Control experiments were performed to elucidate the mechanism of the reaction (Table 2). It is well known that NBS or NBP can generally participate either in radical or ionic pathways depending on the cleavage of the N–Br bond.¹⁸ When the reaction was conducted in the dark, no influence on the reaction efficiency and yield was observed (entry 2). Addition of the radical scavenger BHT (2,6-di-*tert*-butyl-4-methylphenol) to the reaction mixture under the standard conditions had no obvious effect on the product yield (entry 3). This result suggests that a radical pathway is unlikely.

The *in situ* NMR showed that compound **3a** can be identified from the reaction of **1** with NBP within 15 min (Scheme 2). HRMS spectrometry showed a dominant peak at *m/z* =

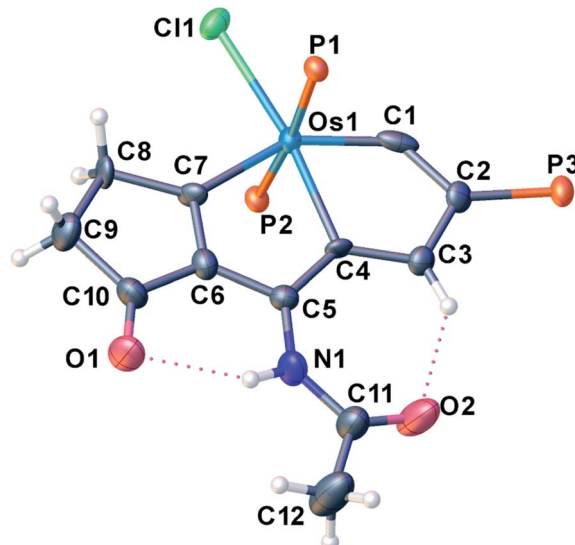
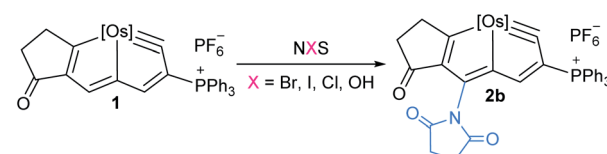


Fig. 3 X-ray crystal structure of the cation of **2c** (thermal ellipsoids are set at the 50% probability level and the phenyl groups in the PPh₃ moieties are omitted for clarity). Selected bond lengths [Å] and angles [°]: Os1–C1: 1.818(10), Os1–C4: 2.146(7), Os1–C7: 2.057(8), C1–C2: 1.411(12), C2–C3: 1.415(11), C3–C4: 1.394(10), C4–C5: 1.411(11), C5–C6: 1.427(11), C6–C7: 1.356(11), C5–N1: 1.387(11), N1H···O1: 2.107, H3···O2: 2.105 C4–Os1–C1: 72.6(3), C7–Os1–C4: 75.7(3).

Table 2 Control experiments^a



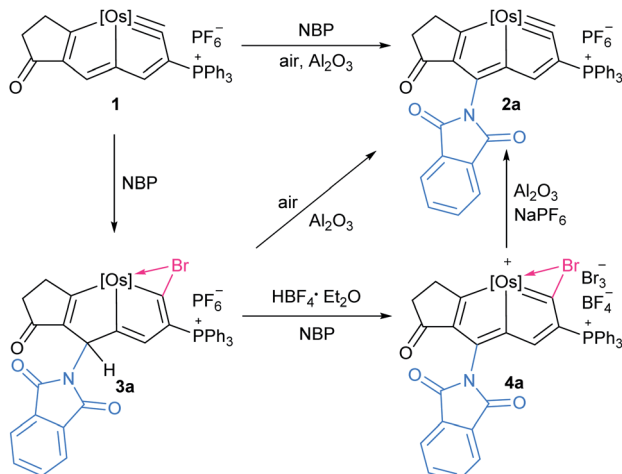
Entry	X	Additive	Yield ^b (%)
1	Br	—	90
2 ^c	Br	—	90
3 ^d	Br	BHT	88
4	I	—	0
5	Cl	—	0 ^e
6	OH	—	0

^a Reaction conditions: **1** (0.20 mmol) with NXS (0.60 mmol) and Al₂O₃ (5.0 mmol) in CH₂Cl₂ (10.0 mL) for 12 h at rt in air. ^b Isolated yield.

^c In the dark. ^d The reaction was carried out in the presence of BHT (1.0 mmol). ^e Only a mixture of unidentified species was detected. [Os] = OsCl(PPh₃)₂.

1380.1864, consistent with the adduct of cationic **1** and NBP [C₇₂H₅₅BrClNO₃OsP₃]⁺ (1380.1855) (see ESI p. S56†). The structure can be inferred from the NMR spectra, which indicates that it is a bromoamidation product with bromide and nitrogen moieties at C1 and C5 positions, respectively. The ¹H NMR spectrum of **3a** displays a signal for the H5 proton at δ = 6.12 ppm determined by ¹H–¹³C heteronuclear single quantum coherence (HSQC) spectroscopy, which is significantly shifted to a higher field when compared to that of **1** (δ = 9.46 ppm). The





Scheme 2 Trapping intermediates **3a** and **4a** in the formation of **2a** from **1**, $[\text{Os}] = \text{OsCl}(\text{PPh}_3)_2$.

signal from C5 ($\delta = 57.5$ ppm) is dramatically shifted upfield when compared to the corresponding resonance observed in **1** ($\delta = 147.0$ ppm) and **2a** ($\delta = 140.3$ ppm). The values strongly support the sp^3 hybridization state of C5. In addition, the H3 proton signal ($\delta = 6.22$ ppm) is also moved upfield compared with that of **1** ($\delta = 8.11$ ppm) and previously reported metalla-pentalenes (*ca.* 7–9 ppm),¹⁹ but is comparable with those observed in osmacyclopentadiene derivatives ($\delta = 6.41$ ppm).²⁰ Notably, the $^{13}\text{C}\{^1\text{H}\}$ NMR and DEPT-135 spectra confirmed the C1 as a quaternary carbon at $\delta = 198.3$ ppm. The chemical shift is upfield compared with those found for related osmacyclopentadienes (*ca.* $\delta = 218$ –235 ppm) due to the bromide attached at C1.^{20,21} The resonances of the two carbonyl carbons in the substituted imide group were observed at $\delta = 169.7$ and 166.2 ppm, respectively. The $^{31}\text{P}\{^1\text{H}\}$ NMR spectrum shows signals from the two phosphorus atoms at $\delta = -22.68$ and -21.11 ppm, respectively. These data all suggest that **3a** is a dearomatization product derived from the 1,5-addition of NBP to **1** (Table 3).

The reaction of **1** with NBS could also give rise to the analogous 1,5-addition product **3b**. Complex **3a** and **3b** could be recognized as the intermediate σ^{H} -adduct in nucleophilic aromatic substitution reactions.²² Strong nucleophiles such as RO^- , H^- , NH_2^- have participated in the formation of the isolated σ^{H} -adducts.²³ It is challenging however for weak nucleophiles such as an imide anion to attack the aromatic ring. The

Table 3 Selected NMR spectroscopic data for the complexes **1**, **2a**, **3a**, **4a**

Compound	$\delta(^1\text{H})$ (ppm)		$\delta(^{13}\text{C})$ (ppm)	
	H3	H5	C1	C5
1	8.11	9.46	324.4	147.0
2a	8.30	—	327.1	140.3
3a	6.22	6.12	198.3	57.5
4a	8.13	—	270.7	151.0

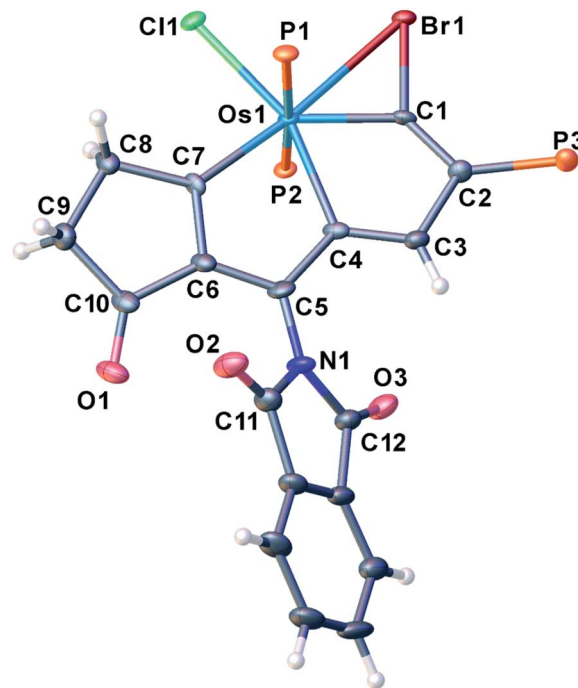


Fig. 4 X-ray crystal structure of the cation of **4a** (thermal ellipsoids are set at the 50% probability level and the phenyl groups in the PPh_3 moieties are omitted for clarity). Selected bond lengths [\AA] and angles [$^\circ$]: Os1–C1: 1.949(5), Os1–C4: 2.146(5), Os1–C7: 2.023(5), Os1–Br1: 2.7241(5), C1–Br1: 1.896(5), C1–C2: 1.366(7), C2–C3: 1.425(7), C3–C4: 1.377(7), C4–C5: 1.414(7), C5–C6: 1.393(7), C6–C7: 1.389(7), C5–N1: 1.379(7), C4–Os1–C1: 68.38(19), C7–Os1–C4: 74.12(19), Os1–C1–Br1: 90.2(2), Br–Os1–C1: 44.10(13), Os1–Br1–C1: 45.67(15).

isolation of a σ^{H} -adduct involving imide anion is limited to extremely electron-deficient aromatics.²⁴

Haloamidation of an unsaturated bond using an electrophilic halogen source such as NBS is an important and well documented synthetic route to vicinal haloamide compounds.²⁵ In contrast, the reactions of amide reagents toward arenes or heteroarenes usually result in either imidation or halogenation.²⁶ In our case, the unique feature of osmapentalyne permits the bromine addition to the Os≡C carbyne, promoting the unusual 1,5-bromoamidation of metallaaromatics. This provides an economical route to access difunctionalized metallacycles.

Treatment of **3a** with excessive amounts of NBP as an oxidant in the presence of $\text{HBF}_4 \cdot \text{Et}_2\text{O}$, led to the formation of the oxidation product **4a** (Scheme 2). The solid-state structure of **4a** was characterized by X-ray single-crystal diffraction (Fig. 4). The bond lengths of Os1–C1 (1.949(5) \AA) and C1–Br1 (1.896(5) \AA) as well as Br1–C1–Os1 bond angle (90.2(2) $^\circ$) are comparable to those of the reported metallabromireniump (1.935 (11) \AA , 1.872(10) \AA and Br1–C7–Os1 95.8(5) $^\circ$, respectively).²⁷ The Os1–Br1 bond length (2.7241(5) \AA) was slightly shorter than that of the reported metallabromireniump (2.8254(12) \AA), demonstrating the stronger interaction between the bromide atom and the metal center. The other metal–carbon bonds, Os1–C4 (2.146(5) \AA) and Os1–C7 (2.023(5) \AA) and the C–C bond lengths



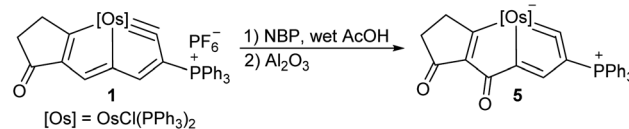
(1.366–1.425 Å) are within the range observed for **2a** and other osmapentalenes,^{19a} suggesting the rearomatization of **4a**. The NMR data are consistent with the crystal structure. In particular, the signal from C1 appears at δ = 270.7 ppm, suggesting the carbene character of C1. This differs from the Os–C single bond observed in **3a** (198.3 ppm). Signals from the remaining ring carbon atoms are observed at δ = 159.8 (C2), 125.4 (C3), 174.1 (C4), 151.0 (C5), 164.3 (C6) and 220.2 (C7) ppm, respectively. The ^1H NMR spectrum of **4a** also shows the signal for H3 at δ = 8.13 ppm in the aromatic region. The singlet peak of the two PPh_3 ligands at δ = –5.11 ppm in the $^{31}\text{P}\{^1\text{H}\}$ NMR spectrum of **4a** reflects the reconstruction of a molecular mirror plane.

Experimentally, *N*-halogen imides other than NBS were used in the reactions (Table 2). No reaction was observed with *N*-iodosuccinimide (NIS), which might only reflect the poor reactivity of *N*-iodoimides (entry 4). When NCS was used in the reaction, a mixture of unidentified species was produced (entry 5). The smaller atomic size of the chlorine atom is known to make it harder to sustain the unsaturated three membered ring due to the imperfect orbital overlap.²⁷ In addition, upon replacement of NBS by *N*-hydroxysuccinimide (NHS), no desired product was observed (entry 6). The bromide cation appears to play a vital role in the reaction.

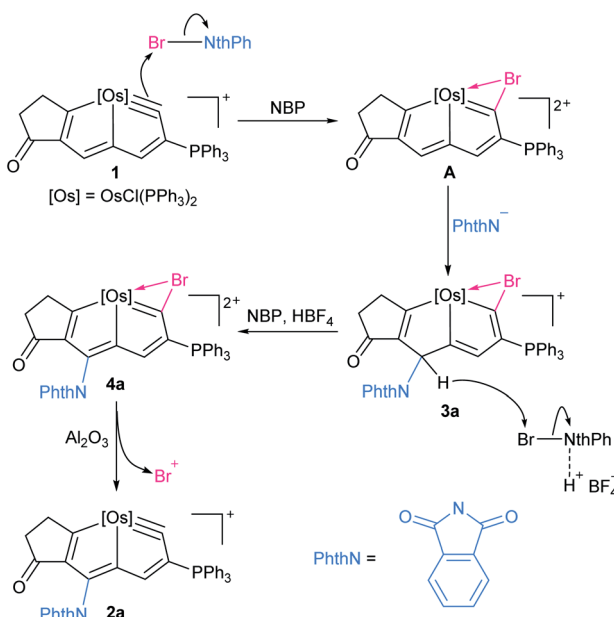
Elimination of the bromine cation from **4a** could generate the osmapentalyne **2a** in high yield upon the addition of Al_2O_3 under an argon atmosphere in the presence of NaPF_6 (Scheme 2). In this context, a reasonable mechanism was proposed for the direct amidation reaction (Scheme 3). Initially, the addition of a bromine cation derived from the *N*-bromoamide to the metal–carbon triple bond produces an extremely electron-deficient cationic metallabromirenium **A**. Subsequently, nucleophilic addition of imide anion afforded the stabilized

intermediate σ^{H} -adduct **3a**, and this is followed by elimination of hydride ion by oxidation to accomplish the $\text{S}_{\text{N}}\text{Ar}$ reaction giving the metallaaromatic product **4a**. Elimination of the bromine cation by Al_2O_3 affords the final amido-substituted product **2a**.

While **1** was reacted with NBP in the presence of wet acetic acid, and then the mixture was treated by aluminium oxide, compound **5** can be isolated in 68% yield (Scheme 4). The X-ray crystallographic analysis confirms it is a new metallacyclic skeleton containing a five-membered metallacycloallene (Fig. 5). Notably, carbonylation at C5 position in **5** was observed rather than *N*-functionalization as in **2**. The proposed mechanism for the formation of **5** showed nucleophilic attack of H₂O to metallabromirenium **A** afforded intermediate **B**, which would be oxidized into carbonyl complex **C**. The cationic **C** is detected by HRMS spectrometry ($m/z = 1249.1461$, [C₆₄H₅₀BrClO₂OSp₃]⁺ calculated $m/z = 1249.1483$) (see ESI p. S62†). The ready elimination of the bromine cation afforded the product **5** containing a metal-vinylidene moiety (see ESI p. S19†). It is presumably that the nucleophilicity of NBP in the presence of the acetic acid is dramatically reduced, thus the C5 position of **1** was prior to being attacked by H₂O. The strategy provides a convenient route to access extraordinary metallacycles with a high degree of skeletal complexity.



Scheme 4 Formation of **5** by reaction of **1** with H_2O , $[\text{Os}] = \text{OsCl}(\text{PPh}_3)_2$.



Scheme 3 Proposed mechanism for the direct amidation of metal-la aromatics, $[\text{Os}] = \text{OsCl}(\text{PPh}_3)_2$.

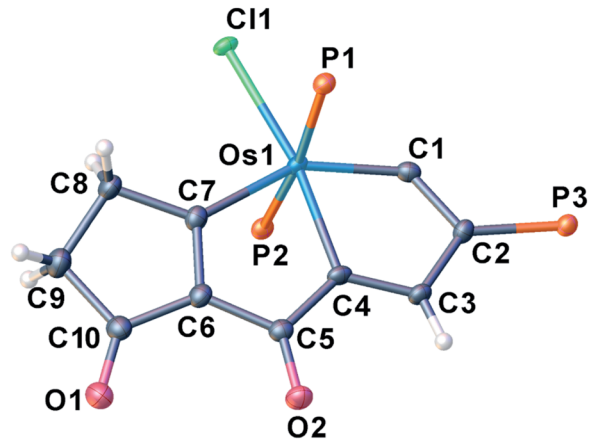
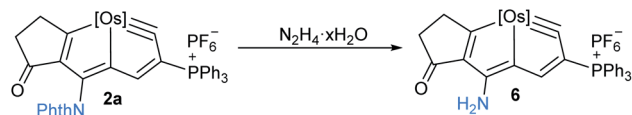


Fig. 5 X-ray crystal structure of **5** (thermal ellipsoids are set at the 50% probability level and the phenyl groups in the PPh_3 moieties are omitted for clarity). Selected bond lengths [\AA] and angles [$^\circ$]: Os1–C4: 2.111(3), Os1–C1: 1.870(3), Os1–C7: 2.059(3), O2–C5: 1.250(3), O1–C10: 1.223(4), C1–C2: 1.374(4), C3–C2: 1.450(4), C4–C3: 1.366(4), C4–C5: 1.465(4), C6–C5: 1.449(4), C6–C7: 1.382(4), C7–C8: 1.512(4), C8–C9: 1.530(4), C10–C9: 1.519(4), C6–C10: 1.464(4), C2–C1–Os1: 130.0(2), C1–C2–C3: 107.3(2), O2–C5–C4: 124.3(3), O1–C10–C6: 129.1(3).



Scheme 5 Transformation of complex **2a** to amino-substituted osmapentalyne **6**, [Os] = OsCl(PPh₃)₂.

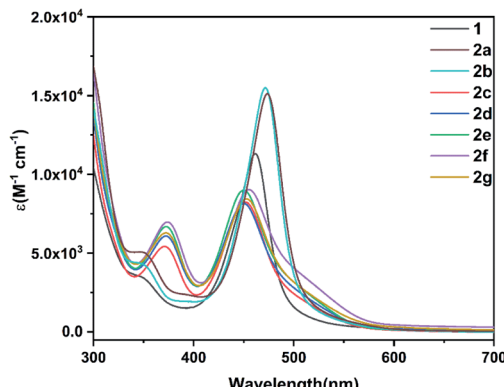


Fig. 6 UV-Vis spectra of osmapentalyne **1** and its *N*-functionalized derivatives **2a**–**2g** (CH₂Cl₂, rt, 5.0 × 10^{−5} M).

Further, transformation of imide product **2a** was performed by treatment of **2a** with hydrazine hydrate, afforded amino-substituted osmapentalyne **6** in high yield (90%) (Scheme 5). Amino-substituted metallaromatics exhibit rich reactivities towards many reagents.¹⁵ Complex **6** represents the first amino-substituted metallapentalyne, which is useful for further functionalization of these unusual metallacyclic compounds.

Thermal stability and spectroscopic properties

The solid state of amidation products **2a**–**2g** can be stored in air at room temperature at least for two weeks. They also exhibit good thermal stability even when heated at 100 °C in air for 5 h (see ESI p. S20†). The UV-Vis absorption spectra of the precursor **1** and its derivatives **2a**–**2g** were investigated. As shown in Fig. 6, compound **1** displays an absorption maximum at $\lambda_{\text{max}} = 460$ nm. The absorption bands for **2a** and **2b**, bearing electron-withdrawing imide groups were observed at approximately $\lambda_{\text{max}} = 472$ nm, slightly red-shifted compared to that of **1**, while **2c**–**2g** with electron-donating amide groups at around $\lambda_{\text{max}} = 450$ nm was slightly blue-shifted. The results show that amidation of metallaaromatic compounds is a feasible methodology with which to subtly tune their photophysical properties.

Conclusions

We have developed a direct and efficient amidation of metallaaromatics, leading to *N*-functionalized osmapentalynes. The successful isolation of the key intermediates, the 1,5-bromoamidation and metallabromireniun species, confirms that the reaction is a three-step process that first involves electrophilic addition, followed by nucleophilic attack and then oxidation.

This study provides insight into a strategy to construct functionalized metallaaromatics and significantly facilitates further exploration of their properties and potential applications.

Author contributions

H. X. and Y.-M. L. conceived the project. H. W. performed the experiments. H. W., Y.-M. L., and Y. R. analyzed and interpreted the experimental data. Y.-M. L. and J. W. drafted the paper. All of the authors discussed the results and contributed to the preparation of the final manuscript.

Conflicts of interest

There are no conflicts to declare.

Acknowledgements

This research was supported by the National Natural Science Foundation of China (No. U1705254, 22071206, 21931002 and 21671164).

Notes and references

- For reviews, see: (a) J. Bariwal and E. Van der Eycken, *Chem. Soc. Rev.*, 2013, **42**, 9283–9303; (b) M.-L. Louillat and F. W. Patureau, *Chem. Soc. Rev.*, 2014, **43**, 901–910; (c) K. Shin, H. Kim and S. Chang, *Acc. Chem. Res.*, 2015, **48**, 1040–1052; (d) Y. Park, Y. Kim and S. Chang, *Chem. Rev.*, 2017, **117**, 9247–9301; (e) R. K. Rit, M. Shankar and A. K. Sahoo, *Org. Biomol. Chem.*, 2017, **15**, 1282–1293.
- For recent examples, see: (a) X. Hu, G. Zhang, L. Nie, T. Kong and A. Lei, *Nat. Commun.*, 2019, **10**, 5467; (b) H. J. Kim, J. Kim, S. H. Cho and S. Chang, *J. Am. Chem. Soc.*, 2011, **133**, 16382–16385; (c) A. A. Kantak, S. Potavathri, R. A. Barham, K. M. Romano and B. DeBoef, *J. Am. Chem. Soc.*, 2011, **133**, 19960–19965; (d) R. Shrestha, P. Mukherjee, Y. Tan, Z. C. Litman and J. F. Hartwig, *J. Am. Chem. Soc.*, 2013, **135**, 8480–8483; (e) K. Foo, E. Sella, I. Thomé, M. D. Eastgate and P. S. Baran, *J. Am. Chem. Soc.*, 2014, **136**, 5279–5282; (f) T. Yamaguchi, E. Yamaguchi and A. Itoh, *Org. Lett.*, 2017, **19**, 1282–1285; (g) K. Sun, Y. Li and Q. Zhang, *Sci. China: Chem.*, 2015, **58**, 1354–1358.
- (a) R. A. Lidgett, E. R. Lynch and E. B. McCall, *J. Chem. Soc.*, 1965, 3754–3759; (b) J. C. Day, M. G. Katsaros, W. D. Kocher, A. E. Scott and P. S. Skell, *J. Am. Chem. Soc.*, 1978, **100**, 1950–1951; (c) L. Stella, *Angew. Chem., Int. Ed. Engl.*, 1983, **22**, 337–350; (d) U. Lüning and P. S. Skell, *Tetrahedron*, 1985, **41**, 4289–4302.
- (a) T. Xiong and Q. Zhang, *Chem. Soc. Rev.*, 2016, **45**, 3069–3087; (b) M. D. Kärkäs, *ACS Catal.*, 2017, **7**, 4999–5022; (c) L. J. Allen, P. J. Cabrera, M. Lee and M. S. Sanford, *J. Am. Chem. Soc.*, 2014, **136**, 5607–5610; (d) H. Kim, T. Kim, D. G. Lee, S. W. Roh and C. Lee, *Chem. Commun.*, 2014, **50**, 9273–9276; (e) S. C. Cosgrove, J. M. C. Plane and S. P. Marsden, *Chem. Sci.*, 2018, **9**, 6647–6652; (f) L. Song, L. Zhang, S. Luo and J.-P. Cheng, *Chem.-Eur. J.*, 2014, **20**,



14231–14234; (g) T. Kuribara, M. Nakajima and T. Nemoto, *Org. Lett.*, 2020, **22**, 2235–2239.

5 For reviews, see: (a) D. Chen, Y. Hua and H. Xia, *Chem. Rev.*, 2020, **120**, 12994–13086; (b) B. J. Frogley and L. J. Wright, *Chem.-Eur. J.*, 2018, **24**, 2025–2038; (c) W. Ma, C. Yu, T. Chen, L. Xu, W.-X. Zhang and Z. Xi, *Chem. Soc. Rev.*, 2017, **46**, 1160–1192; (d) G. Jia, *Acc. Chem. Res.*, 2004, **37**, 479–486; (e) J. R. Bleeke, *Acc. Chem. Res.*, 2007, **40**, 1035–1047; (f) L. J. Wright, *Dalton Trans.*, 2006, 1821–1827; (g) C. W. Landorf and M. M. Haley, *Angew. Chem., Int. Ed.*, 2006, **45**, 3914–3936; (h) C. Zhu and H. Xia, *Acc. Chem. Res.*, 2018, **51**, 1691–1700.

6 (a) M. A. Esteruelas, A. B. Masamunt, M. Oliván, E. Oñate and M. Valencia, *J. Am. Chem. Soc.*, 2008, **130**, 11612–11613; (b) T. Bolaño, R. Castarlenas, M. A. Esteruelas and E. Oñate, *J. Am. Chem. Soc.*, 2006, **128**, 3965–3973; (c) P. Barrio, M. A. Esteruelas and E. Oñate, *J. Am. Chem. Soc.*, 2004, **126**, 1946–1947.

7 (a) J. R. Bleeke, P. Putprasert, T. Thananatthanachon and N. P. Rath, *Organometallics*, 2008, **27**, 5744–5747; (b) V. Jacob, C. W. Landorf, L. N. Zakharov, T. J. R. Weakley and M. M. Haley, *Organometallics*, 2009, **28**, 5183–5190.

8 (a) B. J. Frogley and L. J. Wright, *Angew. Chem., Int. Ed.*, 2017, **56**, 143–147; (b) C. Zhu, S. Li, M. Luo, X. Zhou, Y. Niu, M. Lin, J. Zhu, Z. Cao, X. Lu, T. Wen, Z. Xie, P. V. Schleyer and H. Xia, *Nat. Chem.*, 2013, **5**, 698–703; (c) W. Ruan, T.-F. Leung, C. Shi, K. H. Lee, H. H. Y. Sung, I. D. Williams, Z. Lin and G. Jia, *Chem. Sci.*, 2018, **9**, 5994–5998; (d) J. Chen, K.-H. Lee, H. H. Y. Sung, I. D. Williams, Z. Lin and G. Jia, *Angew. Chem., Int. Ed.*, 2016, **55**, 7194–7198.

9 (a) Z. Huang, Y. Zheng, W.-X. Zhang, S. Ye, L. Deng and Z. Xi, *Angew. Chem., Int. Ed.*, 2020, **59**, 14394–14398; (b) C. Yu, M. Zhong, Y. Zhang, J. Wei, W. Ma, W.-X. Zhang, S. Ye and Z. Xi, *Angew. Chem., Int. Ed.*, 2020, **59**, 19048–19053; (c) Y. Zheng, C.-S. Cao, W. Ma, T. Chen, B. Wu, C. Yu, Z. Huang, J. Yin, H.-S. Hu, J. Li, W.-X. Zhang and Z. Xi, *J. Am. Chem. Soc.*, 2020, **142**, 10705–10714.

10 (a) Á. Vivancos, M. Paneque, M. L. Poveda and E. Álvarez, *Angew. Chem., Int. Ed.*, 2013, **52**, 10068–10071; (b) P. Lara, M. Paneque, M. L. Poveda, L. L. Santos, J. E. Valpuesta, E. Carmona, S. Moncho, G. Ujaque, A. Lledos, E. Alvarez and K. Mereiter, *Chem.-Eur. J.*, 2009, **15**, 9034–9045; (c) M. Paneque, M. L. Poveda, N. Rendón and K. Mereiter, *J. Am. Chem. Soc.*, 2004, **126**, 1610–1611.

11 (a) M. Kuno, K. Suzuki, T. Nakamura and M. Yamashita, *Organometallics*, 2020, **39**, 4139–4142; (b) T. Nakamura, K. Suzuki and M. Yamashita, *J. Am. Chem. Soc.*, 2017, **139**, 17763–17766; (c) T. Nakamura, K. Suzuki and M. Yamashita, *J. Am. Chem. Soc.*, 2014, **136**, 9276–9279; (d) A. J. Ashe III, T. R. Diephouse and M. Y. Elsheikh, *J. Am. Chem. Soc.*, 1982, **104**, 5693–5699; (e) A. J. Ashe III, *Organometallics*, 2009, **28**, 4236–4248.

12 (a) M. Saito, M. Sakaguchi, T. Tajima, K. Ishimura, S. Nagase and M. Hada, *Science*, 2010, **328**, 339–342; (b) M. Nakada, T. Kuwabara, S. Furukawa, M. Hada, M. Minoura and M. Saito, *Chem. Sci.*, 2017, **8**, 3092–3097; (c) J. B. Chen, V. G. Young and R. J. Angelici, *J. Am. Chem. Soc.*, 1995, **117**, 6362–6363.

13 (a) V. C. Arias-Coronado, R. Pereira-Cameselle, A. Ozcelik, M. Talavera, A. Peña-Gallego, J. L. Alonso-Gómez and S. Bolaño, *Chem.-Eur. J.*, 2019, **25**, 13496–13499; (b) M. Talavera, A. Peña-Gallego, J. L. Alonso-Gómez and S. Bolaño, *Chem. Commun.*, 2018, **54**, 10974–10976; (c) C. S. Chin, H. Lee and M.-S. Eum, *Organometallics*, 2005, **24**, 4849–4852; (d) C. S. Chin and H. Lee, *Chem.-Eur. J.*, 2004, **10**, 4518–4522.

14 (a) W. Y. Hung, B. Liu, W. Shou, T. B. Wen, C. Shi, H. H. Sung, I. D. Williams, Z. Lin and G. Jia, *J. Am. Chem. Soc.*, 2011, **133**, 18350–18360; (b) C. E. F. Rickard, W. R. Roper, S. D. Woodgate and L. J. Wright, *Angew. Chem., Int. Ed.*, 2000, **39**, 750–752; (c) B. J. Frogley, A. F. Dalebrook and L. J. Wright, *Organometallics*, 2016, **35**, 400–409.

15 B. J. Frogley, L. C. Perera and L. J. Wright, *Chem.-Eur. J.*, 2018, **24**, 4304–4309.

16 (a) T. Wang, S. Li, H. Zhang, R. Lin, F. Han, Y. Lin, T. B. Wen and H. Xia, *Angew. Chem., Int. Ed.*, 2009, **48**, 6453–6456; (b) T. Wang, H. Zhang, F. Han, L. Long, Z. Lin and H. Xia, *Chem.-Eur. J.*, 2013, **19**, 10982–10991; (c) F. Han, T. Wang, J. Li, H. Zhang and H. Xia, *Chem.-Eur. J.*, 2014, **20**, 4363–4372.

17 (a) C. Zhu, Y. Yang, J. Wu, M. Luo, J. Fan, J. Zhu and H. Xia, *Angew. Chem., Int. Ed.*, 2015, **54**, 7189–7192; (b) Q. Zhuo, J. Lin, Y. Hua, X. Zhou, Y. Shao, S. Chen, Z. Chen, J. Zhu, H. Zhang and H. Xia, *Nat. Commun.*, 2017, **8**, 1912; (c) S. Chen, L. Liu, X. Gao, Y. Hua, L. Peng, Y. Zhang, L. Yang, Y. Tan, F. He and H. Xia, *Nat. Commun.*, 2020, **11**, 4651.

18 (a) Z. Wang, L. Lin, P. Zhou, X. Liu and X. Feng, *Chem. Commun.*, 2017, **53**, 3462–3465; (b) Y. Cai, X. Liu, Y. Hui, J. Jiang, W. Wang, W. Chen, L. Lin and X. Feng, *Angew. Chem., Int. Ed.*, 2010, **49**, 6160–6164; (c) Y.-Y. Yeung, X. Gao and E. J. Corey, *J. Am. Chem. Soc.*, 2006, **128**, 9644–9645; (d) W. Z. Yu, F. Chen, Y. A. Cheng and Y.-Y. Yeung, *J. Org. Chem.*, 2015, **80**, 2815–2821.

19 (a) C. Zhu, C. Yang, Y. Wang, G. Lin, Y. Yang, X. Wang, J. Zhu, X. Chen, X. Lu, G. Liu and H. Xia, *Sci. Adv.*, 2016, **2**, e1601031; (b) C. Zhu, Y. Yang, M. Luo, C. Yang, J. Wu, L. Chen, G. Liu, T. Wen, J. Zhu and H. Xia, *Angew. Chem., Int. Ed.*, 2015, **54**, 6181–6185.

20 M. Luo, Z. Deng, Y. Ruan, Y. Cai, K. Zhuo, H. Zhang and H. Xia, *Organometallics*, 2019, **38**, 3053–3059.

21 J. Chen, Z.-A. Huang, Y. Hua, H. Zhang and H. Xia, *Organometallics*, 2015, **34**, 340–347.

22 (a) M. Mąkosza and K. Wojciechowski, *Chem. Rev.*, 2004, **104**, 2631–2666; (b) M. Mąkosza, *Chem. Soc. Rev.*, 2010, **39**, 2855–2868; (c) V. N. Charushin and O. N. Chupakhin, *Mendeleev Commun.*, 2007, **17**, 249–254; (d) O. N. Chupakhin and V. N. Charushin, *Tetrahedron Lett.*, 2016, **57**, 2665–2672.

23 (a) G. R. Clark, L. A. Ferguson, A. E. McIntosh, T. Sohnle and L. J. Wright, *J. Am. Chem. Soc.*, 2010, **132**, 13443–13452; (b) F. Kloss, V. Krchnak, A. Krchnakova, S. Schieferdecker, J. Dreisbach, V. Krone, U. Mollmann, M. Hoelscher and M. J. Miller, *Angew. Chem., Int. Ed.*, 2017, **56**, 2187–2191; (c)



T. Lemeck, M. Makosza, D. S. Stephenson and H. Mayr, *Angew. Chem., Int. Ed.*, 2003, **42**, 2793–2795; (d) H. C. Van der Plas, V. N. Charushin and B. Van Veldhuizen, *J. Org. Chem.*, 1983, **48**, 1354–1357.

24 (a) I. V. Borovlev, O. P. Demidov, N. A. Kurnosova, G. A. Amangasieva and E. K. Avakyan, *Chem. Heterocycl. Compd.*, 2015, **51**, 170–175; (b) M. K. Stern and B. K. Cheng, *J. Org. Chem.*, 1993, **58**, 6883–6888.

25 (a) A. Alix, C. Lalli, P. Retailleau and G. Masson, *J. Am. Chem. Soc.*, 2012, **134**, 10389–10392; (b) L. Song, S. Luo and J.-P. Cheng, *Org. Lett.*, 2013, **15**, 5702–5705; (c) M. Li, H. Yuan, B. Zhao, F. Liang and J. Zhang, *Chem. Commun.*, 2014, **50**, 2360–2363.

26 Imidation: see ref. 4. Halogenation: (a) G. K. S. Prakash, T. Mathew, D. Hoole, P. M. Esteves, Q. Wang, G. Rasul and G. A. Olah, *J. Am. Chem. Soc.*, 2004, **126**, 15770–15776; (b) F. Mo, J. M. Yan, D. Qiu, F. Li, Y. Zhang and J. Wang, *Angew. Chem., Int. Ed.*, 2010, **49**, 2028–2032; (c) Y. Nishii, M. Ikeda, Y. Hayashi, S. Kawauchi and M. Miura, *J. Am. Chem. Soc.*, 2020, **142**, 1621–1629; (d) S. Duan, J. Turk, J. Speigle, J. Corbin, J. Masnovi and R. J. Baker, *J. Org. Chem.*, 2000, **65**, 3005–3009; (e) M. De Rosa, G. Cabrera Nieto and F. Ferrer Gago, *J. Org. Chem.*, 1989, **54**, 5347–5350.

27 M. Luo, C. Zhu, L. Chen, H. Zhang and H. Xia, *Chem. Sci.*, 2016, **7**, 1815–1818.

